arXiv:1612.08687v1 [cond-mat.mes-hall] 27 Dec 2016

Topological protected defect modes in photonic crystal with a second Chern number

Xiao Zhang,[1,*] You Jian Chen,[1] Bochen Guan,[2] Jun Yu Lin,[1,3] Nai Chao Hu,[1] and Ching Hua Lee[4]

[1] *School of Physics, Sun Yat-sen University, Guangzhou 510275, China*
[2] *Department of Electrical and Computer Engineering, University of Wisconsin, Madison, WI 53706, USA*
[3] *Yat-Sen School, Sun Yat-sen University, Guangzhou 510275, China*
[4] *Institute of High Performance Computing, 138632, Singapore*

(Dated: December 28, 2016)

In the recent years, there has been a drive towards the realization of topological phases beyond conventional electronic materials, including phases defined in more than three dimensions. Photonic crystals are particularly suitable for this purpose since they can be relatively easily fabricated into a wide variety of shapes with macroscopic dimensions. We propose a way to realize 1st and 2nd Chern number topological phases with photonic crystals simply made up of defect resonators embedded within a regular lattice of resonators. Through quasiperiodic spatial modulations in the defect radii, the defect lattice can be described by a direct product of effective Hofstadter models possessing topologically nontrivial Chern bands living in four-dimensional synthetic space. Such photonic systems can be easily experimentally realized with regular photonic crystals consisting of dielectric rods in air, with topological signature measurable from kinks in the transmission spectrum caused by spectrally pumped edge states. Such topologically protected defect modes have potential applications due to their immunity towards small perturbations.

INTRODUCTION

Topological phases like quantum Hall systems [1–3], topological insulators[4–8] and quantum anomalous Hall materials [9–12] rank amongst the most intensely studied topics in condensed matter physics, material science and electrical engineering communities[13, 14]. In these systems, each energy band is ascribed a topological index that mandate the presence interesting boundary states and quantized response. Soon after the discovery of such topological phases in electronic condensed matter systems, analogs in phononic (acoustic) [15–28] systems, photonic systems [29–44] or their hybrid[45] have been proposed and in some cases realized experimentally. Although topological phases with nontrivial Chern invariant in principle exist in any even number of dimensions, physical real space is limited by three dimensions. Hence all conventional topological Chern systems in two or three dimensions, i.e. quantum anomalous Hall materials, Weyl semimetals[46, 47] and their photonic analogs [29, 30, 35, 36, 40–42, 44] can only be characterized by the first Chern number. Topological phases characterized by the second Chern number, dubbed four dimensional (4d) quantum Hall systems[48] cannot be realized in 3d physical space, and have for a long time been believed to exist only in theory.

Recently, it was realized that such second Chern number phases can be realized in photonic systems through synthetic dimensions. Proposals include uni-directional propagating waveguides with aperiodic structures[49] and optical fibers of Weyl materials with helical structure[50]. In the former, the synthetic dimensions arise through the identification of an aperiodic hamiltonian with a Hofstadter lattice containing twice the number of dimensions[51–56]. While first Chern number edge states have been experimentally observed in 1d analogs of such propagating waveguides[40], the experimental realization of their 2d (second Chern number) analogs remain elusive. As such, in this paper we propose an alternative realization of a second Chern number state that is based on conventional photonic crystals (PCs), which is highly desirable due to its maturity in experimental setup.

Meanwhile, defect modes embedded in PC [57–63] are mid-gap states whose resonant frequency can be modulated through their size[64]. They are important in many applications[65–68], but are fragile to perturbations. Small amounts of disorder in such lattice structures can lead to significant detuning of the resonance frequency as well as mode volume of defect modes. A solution for the protection of such defect modes has been recently proposed based on topological crystalline symmetry[65].

In this work, we construct topologically protected defect modes in a regular two dimensional (2d) PC by simply aperiodically modulating the resonator's sizes. This aperiodic PC is described by an effective tight-binding Hamiltonian corresponding to the tensor product of two Hofstadter models with irrational fluxes. The resultant bandstructure assumes a fractal form, and can be characterized by the second Chern number in the space of synthetic dimensions. To motivate our approach, we begin by illustrating the mid-gap defect modes protected by the first Chern number, in a one dimensional (1d) resonator lattice embedded in a 2d PC. The protected defect modes, localized at the end of the 1d lattice, can be viewed as boundary modes in a 2d synthetic space. Next we generalize to a 2d modulated resonator lattice in a 2d PC, and achieve mid-gap defect modes protected by the second Chern number. These protected defect modes

are now boundary modes in a 4d synthetic space. Our calculations are performed by exactly solving Maxwell equations via the finite element method (FEM) with the Maxwell Equation solver COMSOL. Finally we propose a simple experimental setup in the microwave wavelength window, with a proposed PC structure of centimeter size, and which can be easily manufactured with modern fabrication technology.

TIGHT-BINDING HAMILTONIAN OF A 1D RESONATOR LATTICE

To begin with, we give a pedagogical description of the defect modes in 2d PC using a tight-binding (TB) Hamiltonian. First we convert Maxwell's equation to a tight-binding Hamiltonian in the basis of defect modes[69] (Fig 1):

$$H|\psi\rangle = \begin{bmatrix} 0 & i\varepsilon_0^{-1}\vec{\nabla}\times \\ -i\mu_0^{-1}\vec{\nabla}\times & 0 \end{bmatrix} \begin{bmatrix} \vec{E} \\ \vec{H} \end{bmatrix} = \omega|\psi\rangle \qquad (1)$$

where $|\psi\rangle = \begin{bmatrix} \vec{E} \\ \vec{H} \end{bmatrix}$ denotes an eigenmode with eigenfrequency ω. $\varepsilon_0(x, y)$ is a function of the refractive index in real space. Our PC consists of a lattice of equally spaced rods of dielectric constant 10 and radius $0.2a$ separated by air, where a is the lattice spacing. Embedded in this 2d PC is a 1d resonator chain in the x direction made up of rods with radius smaller than $0.2a$, each separated by 2 regular rods (Fig. 1c).

Fig. 1 shows the solution to the Maxwell's equation in the 1d resonator chain. For the TM modes, the 2d PC regular rods form a gapped bulk state which can seen as the "vacuum" surrounding the near-flat defect mode appearing in the mid-gap (Fig. 1a). The defect mode is a resonator confined electromagnetic mode(Fig. 1c), which can be viewed as a photonic analog to an orbital wave function of an atom. Collectively they form the TB basis of the effective Hamiltonian of the PC. Thus we will be able to describe the defect modes with a TB model[69, 70] consisting of the on-site energy ω at every site i, and hopping amplitude t between nearest neighborhood sites i, j:

$$H = \sum_i \omega|\psi_i\rangle\langle\psi_i| + \sum_{\langle i,j\rangle} t|\psi_i\rangle\langle\psi_j| \qquad (2)$$

Further hoppings can be neglected as the defect modes are well-localized.

It is worth mentioning that the qualitative nature of the defect modes can be tuned by adjusting the defect rod radius. For different range of radii, it can admit s, p, d type orbitals[64]. For simplicity, in this work we shall only consider s-type of defect modes arising from rods with radius $r < 0.2a$. The defect band depends on the radius of the defect rod. Fig. 1b shows that the frequency of the defect mode is a monotonic function of the radius of the defect rod.

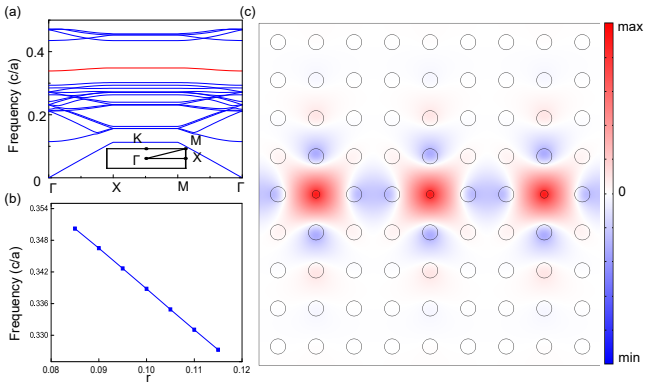

FIG. 1. (a) The frequency bands for the TM modes of our PC consisting of a 2d lattice of radius $r = 0.2a$ rods. Embedded within it is a linear array of defect rods with radius $r = 0.1a$ that replaces one in three regular rods. The dielectric constant is 10. The defect state (red) lies in the large band gap of bulk states (blue). (b) The monotonic dependence of the frequency of the defect state at the Γ point and the radius of defect rods. (c) The distribution of the z component of the electric field strength of the defect states at the Γ point. It decays rapidly away from the line of defects.

DEFECT MODES PROTECTED BY THE FIRST CHERN NUMBER

To realize PC defect states that are protected by the first Chern number, we simply modulate the size of the resonators such that we obtain an effective Hofstadter model[40, 53]. Here we illustrate the simple example of 1d defect modes protected by the first Chern number shown in (Fig. 2). We construct this defect lattice using a similar setup as Fig. 1, but modulate the radius of the resonators instead of keeping them constant:

$$r = r_0 + r_1 \cos(2\pi bx + \phi_x), \qquad (3)$$

where x labels the resonators in the $\hat{x}$ direction and b is an irrational number. A synthetic dimension is implemented through the parameter ϕ_x, which sets the radius of the first defect. From Fig. 2, the bandstructure (for $b = (1+\sqrt{5})/2$) consists of a fractal hierarchy of bulk bands. Upon varying ϕ_x over a period, edge states are seen to continuously connect the bulk bands. To understand the topological origin of these mid-gap states, one refers to the effective TB Hamiltonian

$$\begin{aligned} H = &\sum_x \lambda \cos(2\pi bx + \phi_x)|\psi_x\rangle\langle\psi_x| \\ &+ \sum_{x,x+1} V_{x,x+1}(\phi)|\psi_x\rangle\langle\psi_{x+1}| \\ &+ \sum_{x,x-1} V_{x,x-1}(\phi)|\psi_x\rangle\langle\psi_{x-1}| \end{aligned} \qquad (4)$$

which follows from the form of the quasiperiodic modulation in the defect radius (Eq. 1). In the s-wave approximation, $V_{x,x\pm1} \approx V_0$ are constant to leading order, and further hoppings can be dropped. Hence we recover a variation of the 1d Aubry-André (AA) model[71]. Eq. 4 can be mapped to a 2d integer quantum Hall system by reinterpreting the modes $|\psi_x\rangle$ as Landau gauge wavefunctions on a 2d lattice. If we also reinterpret ϕ_x as a momentum variable $k_x a$, Eq. 4 becomes the Hofstadter Hamiltonian given by $H|\psi_{x,k}\rangle = V_0(|\psi_{x+1,k} + |\psi_{x-1,k}) + \lambda\cos(2\pi bx + k_x a)|\psi_x\rangle$. This is just the hopping Hamiltonian on a rectangular lattice with horizontal and vertical hoppings V_0 and $\lambda/2$, and $2\pi b$ flux threaded per plaquette, i.e. a quantum Hall system on a lattice. By taking a rational approximation to the flux $b \approx p/q$ where p and q are relatively prime, this hopping Hamiltonian also describes a Chern insulator with q bands, each with Chern numbers detailed as in Ref. 51. In the irrational limit, q diverges and the bands tend towards perfectly flat 'Landau levels'[72].

Viewed as a Chern insulator, the midgap states are just the topological edge states corresponding to the bulk chiral anomalies[73]. Physically, they realize the pumping mechanism in Laughlin's spectral flow argument, even though in this context it is the defect modes and not electrons that are pumped. These midgap states exist at the edge (ends) of the defect line, as is evident in Fig. 2c), and are pumped from one end to the other as the midgap state traverse a gap[74–76]. The number of states pumped over a period of ϕ_x within a gap depends on the difference in the combined Chern numbers of the bands on either side of gap.

For our FEM solution to Maxwell's equations, we take 21 resonators in a 1d super-cell. As illustrated in Fig. 2a, when we apply a periodic boundary condition for the super-cell, which means we repeat the super-cell structure in x direction, we can see bulk bands separated by band gaps in the 1d Brillouin zone (BZ) of ϕ_x (Fig. 2a). However, if we take an open boundary condition in the x direction, which means the that left and right sides of the super-cell are terminated with regular dielectric rods in the bulk (Fig. 2c), we see the boundary states (Fig. 2b) localized on the end of defect chain , whose field distribution is shown in Fig. 2c.

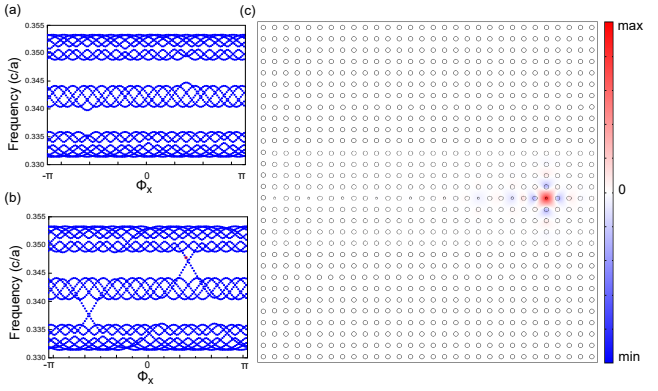

FIG. 2. (a) The frequency bandstructure of the defect states for a 1d PC resonator lattice embedded in a regular periodic 2d PC, as a function of ϕ_x. The radius of the defect rods obeys Eq.3 with parameters $r_0 = 0.101569a$, $r_1 = -0.012569a$ and $b = \frac{1+\sqrt{5}}{2}$. The FEM is performed with a repeated (periodic boundary condition) super-cell having 21 defect rods. (b) The frequency bands of defect states for a 1d PC resonator lattice with open boundary condition as a function of ϕ_x. There is only one super-cell terminated by regular bulk dielectric rods on both ends. (c) The z direction electric field strength (E_z)distribution of the localized defect boundary state at $\phi_x = 1.25$ and $\omega = 0.3480(c/a)$ (red circle in (b)) with open boundary conditions.

DEFECT MODES PROTECTED BY THE SECOND CHERN NUMBER

We now come to the main results of this paper, which involves extending the array of defect rods to a 2d defect lattice within a 2d lattice of regular rods, the "vacuum".

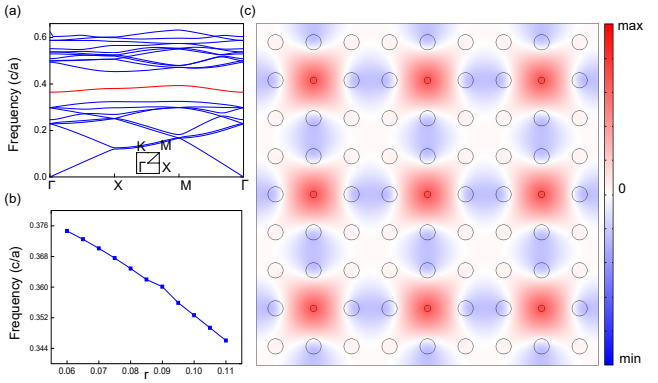

FIG. 3. Defect states before adding quasiperiodic modulation: (a) The frequency bands for PC of TM modes with $r = 0.2a$ regular rods forming the "vacuum", with a 2d array of $r = 0.85a$ defect rods embedded within it. The dielectric constant is 8. The defect state (red) lies in the large band gap of bulk states (blue). (b) The monotonic relation between the frequency of defect state at Γ point and the radius of defect rod. (c) The distribution of the z component of electric field strength of the defect state at the Γ point.

To realize PC defect states protected by the second Chern number, we modulate the radius of the defect rods shown in (Fig. 4), in direct generalization of the first Chern number defect lattice construction:

$$r = r_0 + r_x \cos(2\pi bx + \phi_x) + r_y \cos(2\pi bx + \phi_y). \quad (5)$$

where the tuple x and y describes a resonator located on the $3x^{th}$ row and $3y^{th}$ column. b is a irrational number which we keep as $(1+\sqrt{5})/2$. The synthetic dimension parameters ϕ_x and ϕ_y sets the radius for the first defect, which is given by $r_0 + \cos\phi_x + \cos\phi_t$. The defect states are numerically solved with the FEM method with an 8×8 resonator 2d super-cell. In Fig. 4a, when we apply a periodic boundary condition for the super-cell, which means we repeat the super-cell structure in x and y direction, we can see two band gaps in the 2d BZ of ϕ_x and ϕ_y (Fig. 4a). However, if we take an open boundary condition in x and y direction, which means the surrounding of the super-cell is terminated with regular dielectric rods constituting the bulk (Fig. 4c). Then we see the boundary states appearing in the gap (Fig. 4b), whose field distribution is shown in Fig. 4c.

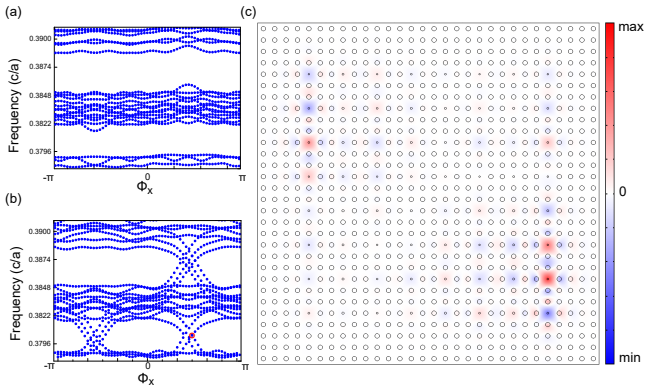

FIG. 4. (a) and (b): The frequency bands of the defect states of our 2d modulated PC resonator lattice embedded in a regular 2d PC, computed with periodic and open boundary conditions respectively. They are plotted as a function of modulation offset parameter ϕ_x, with ϕ_y set to 0. The radius of the defect rods obeys Eq.5 with parameters $r_0 = 0.085204a$, $r_1 = r_2 = -0.01017a$ and $b = \frac{1+\sqrt{5}}{2}$. For a), The Maxwell's equation is solved with the FEM is performed with a repeated (periodic boundary condition) super-cell having 64 defect rods with $n = 8$ along x and y. (c) The z direction electric field strength (E_z) distribution of the defect boundary state at $\phi_x = 1.5$ and $\omega = 0.3806(c/a)$ (red circle in (b)) with open boundary conditions. The defect states are evidently localized at the edge in both x and y directions, with the directional asymmetry in decay length arising from the inequivalence of ϕ_x and ϕ_y.

To understand the nature of the defect edge modes, we write down the effective Hamiltonian which should be of the form

$$\begin{aligned} H = &\sum_{x,y} \omega_{(x,y)}(\phi_x,\phi_y) \left|\psi_{(x,y)}\right\rangle \left\langle\psi_{(x,y)}\right| \\ &+ \sum_{x,y} V_{(x,y),(x\pm1,y)}(\phi_x,\phi_y) \left|\psi_{(x,y)}\right\rangle \left\langle\psi_{(x\pm1,y)}\right| \\ &+ \sum_{x,y} V_{(x,y),(x,y\pm1)}(\phi_x,\phi_y) \left|\psi_{(x,y)}\right\rangle \left\langle\psi_{(x,y\pm1)}\right| \end{aligned} \quad (6)$$

where $\omega_{(x,y)}(\phi_x,\phi_y)$, $V_{(x,y),(x\pm1,y)}(\phi_x,\phi_y)$ and $V_{(x,y),(x,y\pm1)}(\phi_x,\phi_y)$ contain modulations proportional to $r_x\cos(2\pi bx+\phi_x) + r_y\cos(2\pi bx+\phi_y)$ (Eq.5). This is just a superposition of two (off-diagonal) Aubry-André models[71] in different directions, with eigenmodes being products of the 1d Aubry-André model eigenmodes.

Upon reinterpreting the basis modes in Eq. 6 as Laudau gauge eigenfunctions, our 2d defect PC lattice can be interpreted as a tensor product of two Hofstadter models, which hence lives in 4d space. This allows for a natural interpretation of its topology as arising from the second Chern number[49, 73]

$$C_2 = \frac{\epsilon_{ijkl}}{32\pi^2} \int Tr[f_{ij} f_{kl}]\, d^4k \quad (7)$$

where $f_{ij} = P\partial_i P \partial_j P$ for i,j synthetic dimensions of the Hofstadter model, and P the projector onto the band of interest. In our case, C_2 is particularly easy to compute, since the product nature of the eigenmodes implies that $Tr(f \wedge f)$ factorizes into two copies of Trf.

EXPERIMENTAL PROPOSAL

We have seen that topological edge states appear within the bulk gaps due to the presence of an effective magnetic flux b which takes the form of defect modulation. Here we describe a simple experimental proposal for realizing these edge states through transmission spectrum measurements in the microwave wavelength window[61–63].

Our PC is made up of a background "vacuum" 2d lattice of rods of dielectric constant 8 with lattice constant $a = 0.113$ m and rod radius $0.2a$. One in every three rods is replaced by a defect rod of the same dielectric constant, but of radius quasiperiodically modulated as per Eq. 5 and Fig. 4. This PC can be easily constructed with conventional PC fabrication processes. It is very easy to fabricate the PC sample with high precision since a is in the decimeter range.

A midgap edge state will appear as a distinct peak in the transmission spectrum when the wavelength is tuned within the bulk gap. From our FEM simulations we have, for instance, the resonant peak $\lambda = 0.2974m$ when $\phi_x = 1.5, \phi_y = 0$. We can also investigate the 1D defect lattice mentioned previously, where $\lambda = 0.2974m$ when $\phi = 1.25$ and $a = 0.104$m.

CONCLUSION

In summary, we have proposed a way to realize 1st and 2nd Chern number topological phases with regular, easily-fabricated photonic crystals with defect resonators (rods) embedded within a regular lattice of resonators. Through quasiperiodic spatial modulations in the defect radii, the defect lattice can be described by a direct product of effective Hofstadter models possessing topologically nontrivial Chern bands. The topological signatures of these bands lie in their edge states, which are seen to traverse the bulk gaps as synthetic dimension parameters ϕ_x, ϕ_y are varied over a period. Such photonic systems can be easily experimentally realized with regular photonic crystals with dielectric rods in air, and we propose experiments realizing our precise predictions from FEM simulations. Those topologically protected defect modes has potential applications due to their immunity to small perturbations.

ACKNOWLEGMENT

Xiao Zhang is support by the National Natural Science Foundation of China (No.11404413) and the Natural Science Foundation of Guangdong Province (No.2015A030313188). Bochen Guan is supported by a scholarship from the Oversea Study Program of Guangzhou Elite Project.

* zhangxiao@mail.sysu.edu.cn

[1] K. von Klitzing, Reviews of Modern Physics **58**, 519 (1986).
[2] K. S. Novoselov, Z. Jiang, Y. Zhang, S. Morozov, H. Stormer, U. Zeitler, J. Maan, G. Boebinger, P. Kim, and A. Geim, Science **315**, 1379 (2007).
[3] J. K. Jain, Physical review letters **63**, 199 (1989).
[4] X.-L. Qi and S.-C. Zhang, Reviews of Modern Physics **83**, 1057 (2011).
[5] M. Z. Hasan and C. L. Kane, Reviews of Modern Physics **82**, 3045 (2010).
[6] B. A. Bernevig, T. L. Hughes, and S.-C. Zhang, Science **314**, 1757 (2006).
[7] H. Zhang, C.-X. Liu, X.-L. Qi, X. Dai, Z. Fang, and S.-C. Zhang, Nature physics **5**, 438 (2009).
[8] X. Zhang, H. Zhang, J. Wang, C. Felser, and S.-C. Zhang, Science **335**, 1464 (2012).
[9] C.-X. Liu, X.-L. Qi, X. Dai, Z. Fang, and S.-C. Zhang, Physical review letters **101**, 146802 (2008).
[10] R. Yu, W. Zhang, H.-J. Zhang, S.-C. Zhang, X. Dai, and Z. Fang, Science **329**, 61 (2010).
[11] C.-Z. Chang, J. Zhang, X. Feng, J. Shen, Z. Zhang, M. Guo, K. Li, Y. Ou, P. Wei, L.-L. Wang, *et al.*, Science **340**, 167 (2013).
[12] M. Ezawa, Physical review letters **109**, 055502 (2012).
[13] X. Zhang, J. Wang, and S.-C. Zhang, Physical Review B **82**, 245107 (2010).
[14] M. Barsoum, H.-I. Yoo, I. Polushina, V. Y. Rud, Y. V. Rud, and T. El-Raghy, Physical Review B **62**, 10194 (2000).
[15] E. Prodan and C. Prodan, Physical review letters **103**, 248101 (2009).
[16] C. Kane and T. Lubensky, Nature Physics **10**, 39 (2014).
[17] R. Süsstrunk and S. D. Huber, Science **349**, 47 (2015).
[18] L. M. Nash, D. Kleckner, A. Read, V. Vitelli, A. M. Turner, and W. T. Irvine, Proceedings of the National Academy of Sciences **112**, 14495 (2015).
[19] Z. Yang, F. Gao, X. Shi, X. Lin, Z. Gao, Y. Chong, and B. Zhang, Physical review letters **114**, 114301 (2015).
[20] Z. Yang, F. Gao, and B. Zhang, arXiv preprint arXiv:1504.02655 (2015).
[21] R. Fleury, A. Khanikaev, and A. Alu, arXiv preprint arXiv:1511.08427 (2015).
[22] A. B. Khanikaev, R. Fleury, S. H. Mousavi, and A. Alù, Nature communications **6** (2015).
[23] P. Wang, L. Lu, and K. Bertoldi, Physical Review Letters **115**, 104302 (2015).
[24] D. Rocklin, S. Zhou, K. Sun, and X. Mao, arXiv preprint arXiv:1510.06389 (2015).
[25] Y. Liu, Y. Xu, S.-C. Zhang, and W. Duan, arXiv preprint arXiv:1606.08013 (2016).
[26] X. Cheng, C. Jouvaud, X. Ni, S. H. Mousavi, A. Z. Genack, and A. B. Khanikaev, Nature materials (2016).
[27] C. He, X. Ni, H. Ge, X.-C. Sun, Y.-B. Chen, M.-H. Lu, X.-P. Liu, and Y.-F. Chen, Nat Phys **advance online publication** (2016), letter.
[28] Z.-Y. Ong and C. H. Lee, Physical Review B **94**, 134203 (2016).
[29] F. Haldane and S. Raghu, Physical review letters **100**, 013904 (2008).
[30] Z. Wang, Y. Chong, J. D. Joannopoulos, and M. Soljačić, Physical review letters **100**, 013905 (2008).
[31] Z. Wang, Y. Chong, J. Joannopoulos, and M. Soljačić, Nature **461**, 772 (2009).
[32] M. C. Rechtsman, J. M. Zeuner, Y. Plotnik, Y. Lumer, D. Podolsky, F. Dreisow, S. Nolte, M. Segev, and A. Szameit, Nature **496**, 196 (2013).
[33] W. Gao, M. Lawrence, B. Yang, F. Liu, F. Fang, B. Béri, J. Li, and S. Zhang, Physical review letters **114**, 037402 (2015).
[34] L.-H. Wu and X. Hu, Phys. Rev. Lett. **114**, 223901 (2015).
[35] L. Lu, L. Fu, J. D. Joannopoulos, and M. Soljačić, Nature Photonics **7**, doi:10.1038 (2013).
[36] L. Lu, Z. Wang, D. Ye, L. Ran, J. D. Fu, Liangand Joannopoulos, and M. Soljačić, Science **349**, 622 (2015).
[37] L. Lu, C. Fang, L. Fu, S. G. Johnson, J. D. Joannopoulos, and M. Soljačić, Nature Physics **12**, 337 (2016), letter.
[38] Y.-L. Xu, W. S. Fegadolli, L. Gan, M.-H. Lu, X.-P. Liu, Z.-Y. Li, A. Scherer, and Y.-F. Chen, Nature Communications **7**, 11319 EP (2016), article.
[39] J. Y. Lin, N. C. Hu, Y. J. Chen, C. H. Lee, and X. Zhang, arXiv preprint arXiv:1607.06524 (2016).
[40] Y. E. Kraus, Y. Lahini, Z. Ringel, M. Verbin, and O. Zilberberg, Physical review letters **109**, 106402 (2012).
[41] M. Verbin, O. Zilberberg, Y. E. Kraus, Y. Lahini, and Y. Silberberg, Physical review letters **110**, 076403 (2013).

[42] Y. E. Kraus and O. Zilberberg, Physical review letters **109**, 116404 (2012).

[43] C. He, X.-C. Sun, X.-P. Liu, M.-H. Lu, Y. Chen, L. Feng, and Y.-F. Chen, Proceedings of the National Academy of Sciences **113**, 4924 (2016).

[44] Y.-G. Peng, C.-Z. Qin, D.-G. Zhao, Y.-X. Shen, and X.-Y. Xu, Nat. Commun. **7**, doi: 10.1038 (2016).

[45] V. Peano, C. Brendel, M. Schmidt, and F. Marquardt, Physical Review X **5**, 031011 (2015).

[46] H. Weng, F. Chen, F. Zhong, B. Bernevig, and X. Dai, Phys. Rev. X **5**, 1 (2015).

[47] S.-Y. Xu, P. y. Belopolski, N. Alidoust, M. Neupane, G. Bian, C.-l. Zhang, R. Sankar, G. Chang, Z. Yuan, C.-C. Lee, S.-M. Huang, Z. Hao, J. Ma, D.-S. Sanchez, W. Baokai, A. Bansil, F. Chou, P.-P. Shibayev, H. Lin, S. Jia, and M. Hasan, Science **349**, 613 (2015).

[48] S.-C. Zhang and J. Hu, Science **294**, 823 (2001).

[49] Y. E. Kraus, Z. Ringel, and O. Zilberberg, Physical review letters **111**, 226401 (2013).

[50] L. Lu and Z. Wang, arXiv preprint arXiv:1611.01998 (2016).

[51] Y. Hatsugai, Physical Review B **48**, 11851 (1993).

[52] C. Dean, L. Wang, P. Maher, C. Forsythe, F. Ghahari, Y. Gao, J. Katoch, M. Ishigami, P. Moon, M. Koshino, *et al.*, Nature **497**, 598 (2013).

[53] K. A. Madsen, E. J. Bergholtz, and P. W. Brouwer, Physical Review B **88**, 125118 (2013).

[54] I. I. Satija, arXiv preprint arXiv:1405.0263 (2014).

[55] D.-T. Tran, A. Dauphin, N. Goldman, and P. Gaspard, Physical Review B **91**, 085125 (2015).

[56] J.-N. Fuchs and J. Vidal, Physical Review B **94**, 205437 (2016).

[57] S.-S. Cheng, L.-M. Li, C. Chan, and Z. Zhang, Phys. Rev. B **59**, 4091 (1999).

[58] S. Noda, A. Chutian, and M. Imada, Nature **407**, 608 (2000).

[59] M. Sigalas, C. M. Soukoulis, E. N. Economou, C. T. Chan, and K. M. Ho, Phys. Rev. B **48**, 14121 (1993).

[60] M. Bayindir, E. Cubukcu, I. Bulu, and E. Ozbay, Phys. Rev. B **63**, 1 (2001).

[61] M. Sigalas, K. Soukoulias, E. E.N., C. Chan, and K. He, Physical review B **48**, 14121 (1993).

[62] C.-J. Jin, B.-Y. Cheng, B.-Y. Man, Z.-L. Li, and D.-Z. Zhang, Physical review B **61**, 10762 (2000).

[63] D. Smith, S. Shultz, S. McCall, and P. Platzman, Journal of Modern Optics **41**, 395 (1994).

[64] P. R. Villeneuve, S. Fan, and J. Joannopoulos, Physical Review B **54**, 7837 (1996).

[65] J. Noh, W.-A. Benalcazar, S. Huang, M.-J. Collins, K. Chen, T.-L. Hughes, and M.-C. Rechtsman, arXiv:1611.02373 (2016).

[66] J.-L. O'Brien, A. Furusawa, and J. Vučaronković acute, Physical Review B **93**, 155155 (2016).

[67] D. Englund, D. Fattal, E. Waks, G. Solomon, B. Zhang, T. Nakaoka, Y. Arakawa, Y. Yamamoto, and J. Vučković, Phys. Rev. Lett. **95**, 013904 (2005).

[68] J. M. Dudley, G. Genty, and S. Coen, Rev. Mod. Phys. **78**, 1135 (2006).

[69] Z. Wang and S. Fan, Applied Physics B **81**, 369 (2005).

[70] Y. Xu, Y. Li, R. K. Lee, and A. Yariv, Phys. Rev. E **62**, 7389 (2000).

[71] S. Aubry and G. André, Ann. Israel Phys. Soc. (1980).

[72] Indeed, an infinite number of bands is required for perfectly flat Chern bands, as can be proven via K-theory[77–79].

[73] X.-L. Qi, T. L. Hughes, and S.-C. Zhang, Physical Review B **78**, 195424 (2008).

[74] Z. Huang and D. P. Arovas, Physical Review B **86**, 245109 (2012).

[75] A. Alexandradinata, X. Dai, and B. A. Bernevig, Physical Review B **89**, 155114 (2014).

[76] C. H. Lee and P. Ye, Physical Review B **91**, 085119 (2015).

[77] L. Chen, T. Mazaheri, A. Seidel, and X. Tang, Journal of Physics A: Mathematical and Theoretical **47**, 152001 (2014).

[78] C. H. Lee, D. P. Arovas, and R. Thomale, Physical Review B **93**, 155155 (2016).

[79] N. Read, arXiv preprint arXiv:1608.04696 (2016).